ASEAN Journal of Chemical Engineering 2023, Vol. 23, No. 2, 240 – 254

Chemical Properties and Breakthrough Adsorption Study of Activated Carbon Derived from Carbon Precursor from Carbide Industry

Nursyuhani Che Husain [1]
Nurul Athirah Zawawi [1]
Fazlena Hamzah [*,1]
Miradatul Najwa Mohd Rodhi [1]
Harumi Veny [1]
Dessy Ariyanti [2]
Nur Athikah Mohidem [3]

[1]*Biocatalysis and Biobased Material Technology Research Group, School of Chemical Engineering, College of Engineering, Universiti Teknologi MARA, UiTM Shah Alam, 40450 Shah Alam, Selangor, Malaysia*

[2]*Department of Chemical Engineering, Faculty of Engineering, Universitas Diponegoro, Tembalang, Semarang, Indonesia*

[3]*Department of Biological and Agricultural, Faculty of Engineering, Universiti Putra Malaysia, Sedang 43400, Selangor, Malaysia*

[*]e-mail: fazlena@uitm.edu.my

Submitted 11 December 2022 *Revised* 7 April 2023 *Accepted* 16 May 2023

Abstract. The residual carbon from the carbide industry in Malaysia has been explored as a precursor in activated carbon (ACs) processing via chemical activation with potassium hydroxide (KOH). The residual carbon from the carbide industry consists of high fixed carbon content and is a sustainable source of raw material, making it a promising precursor for ACs processing. However, the synergy between activation temperature with impregnation ratio has yet to be well explored for precursors from carbide processing. Thus, in the present work, impregnation ratios from 1:1 to 1:5 and temperature for the activation process from 300°C to 700°C were examined in the ACs processing. The impact of these factors was evaluated towards the chemical characteristic of the derived ACs, such as pores and surface morphology, functional groups, and thermal profile. The finding indicated that the ratio of as-received carbon /KOH from 1:1 to 1:5 provided ACs with BET surface areas of 130 – 458 m^2 /g and micropores content of 19 – 25.75%. The results suggested that the highest BET surface area in this range of study was 458.15 m^2 /g at an activation temperature of 700°C and an impregnation ratio of 1:1. Then the developed ACs were further evaluated in carbon dioxide (CO_2) adsorption using breakthrough CO_2 adsorption. The breakthrough time and CO_2 adsorption rate capacity were calculated as 70 s and 0.175 mmol/g, respectively. This finding indicated that as-received carbon precursors from the carbide industry could be explored as one of the potential materials in ACs development, forming the microporous structure during KOH activation and encouraging the binding of CO_2 molecules in CO_2 capture.

Keywords: Activated Carbon, Carbide, Chemical Activation, CO_2 Capture, Impregnation

DOI: 10.22146/ajche.80035

INTRODUCTION

Introduction CO_2 is the most emitted greenhouse gas (GHG) from industrial activities such as fossil fuel use, industrial processes, and product use. According to the report by UN Environmental Program 2020, global GHG emissions continued to grow for the third consecutive year in 2019, reaching a record high of 52.4 $GtCO_2e$ (range: ±5.2) without land-use change (LUC) emissions and 59.1 $GtCO_2e$ (range: ±5.9) when including LUC. The release of greenhouse gases, especially CO_2, has contributed to global weather changes and several other consequences, such as human health and environmental impact. The issue with global warming led to coastal erosion, an incremental temperature that causes an impact on the glaciers and ice sheets capacity, rising sea levels, and extreme changes in global and climate patterns (Hussain et al., 2020). Thus, various approaches have been proposed and explored in capturing and sequestrating CO_2 to tackle this issue for a sustainable future.

ACs have been widely explored in CO_2 capture due to their excellent performance as an adsorbent, variation of the raw material, and simple processing (Jatinder et al., 2019). The excellent attribute of CO_2 adsorbent has strongly relied on the large surface area and micropore volume, favorable pore size distribution, surface chemistry including the oxygen functional groups, the degree of polarity, and the active surface area. As Khalili et al., 2000 and Wang et al., 2007 reported, ACs in gas adsorption must possess pores with effective radii significantly smaller than 16–20 A˚. This special surface and characteristic can be achieved through the activation process, either via thermal or chemical activation. In thermal or physical activation, a carbonaceous precursor will be primarily carbonized at a temperature below 700°C, followed by the activation of the obtained char with oxidizing gases such as air, CO_2, or steam at temperatures of 700 to 1100°C. Chemical activation involves impregnating raw material with chemical agents such as H_3PO_4, $ZnCl_2$, or KOH, followed by carbonization at temperatures between 400 and 800°C under a nitrogen atmosphere (Nahil et al., 2012).

Carbon precursor in ACs synthesis can be obtained from a wide range of carbon-containing materials such as lignocellulose material (Seyyedeh et al., 2020), agriculture waste (Seyyedeh et al., 2021), and waste food (Ramona et al., 2019). The most frequently used raw materials in ACs synthesis are rice husk, corn cobs, bamboo, fruit stone, date stone, almond shell, sugar cane bagasse, coconut shell, palm shell, and cotton stalk. However, more research on industrial waste as a carbon precursor in ACs processing has yet to be explored. Nassima et al., 2018 utilized cotton cloth residue as the precursor in the AC synthesis. Microporous activated carbons from cotton cloth showed high surface area (up to 1175 m^2g^{-1}) and total volume at 0.616 cm^3g^{-1} using an impregnation ratio (mass of H_3PO_4/mass of precursor) of 50% and a pyrolysis temperature of 600°C. As-received carbon from carbide industries is another potential precursor for ACs processing due to the high fixed carbon content (>50%) and material availability. Carbon residue from carbide industries has not been comprehensively studied.

The main objective of the present work is to prepare ACs from as-received carbon from the carbide industry in Malaysia with a highly microporous and large specific surface area that is considered a high potential adsorbent

for CO_2 adsorption. The experimental work is based on the impregnation method and activation of ACs with KOH. The influence of different impregnation ratios of KOH and activation temperature on the pore structure and the CO_2 adsorption capacity of the prepared AC were investigated.

MATERIALS AND METHODS

Materials

Malaysian Carbide Industries, MCB Industries Sdn Bhd, Kemunting Malaysia supplied as-received carbon material. As-received carbon was residue wood carbon (size <10 mm) for carbide processing. The analytical grade of potassium hydroxide (KOH) and hydrochloric acid (HCl) used in the present work was purchased from R&M Chemicals Sdn. Bhd.

Chemical Activation of the Carbon Precursor

As-received carbon precursor was impregnated with 1.0 g/L potassium hydroxide (KOH) at room temperature, using a weight ratio carbon/KOH of 1:1 to 1:5 as Cafer, 2012 reported. The mixture was then heated at 90℃ for 30 minutes and left for 24 hours soaking. Afterward, access KOH was filtered, and impregnated solid carbon was calcinated in the furnace for 2 hours. The activation temperature was varied from 300℃ to 700℃. The calcinated product was cooled to room temperature, washed with 1.0 g/L hydrochloric acid (HCl), and rinsed with distilled water several times until the pH of the activated carbon was reduced to pH 6. Then, the obtained ACs were dried in an oven at 150℃. The produced activated carbon was cooled to room temperature in a desiccator and analyzed using BET surface area (m^2/g), pore distribution (micropore, mesopore) (cm^3/g), Fourier Transform Infrared (FTIR), and Scanning Electron Microscopy (SEM). The overall work of the study is illustrated in Figure 1.

Thermal Analysis

Thermal stability and volatile component composition of the carbon precursor were observed with the changes in the mass once the sample was heated in Thermogravimetric analysis (TGA), Mettler Toledo (TGA 851/1600, Greifensee, Switzerland) analyzer. 19 g of As-received carbon was heated under a nitrogen environment, and the moisture content, volatile matter, ash content, and fixed carbon content was calculated based on mass reduction. In the present work, the sample was heated from room temperature to 700°C at a heating rate of 10°C/min. The fixed carbon content was determined according to Eq. (1):

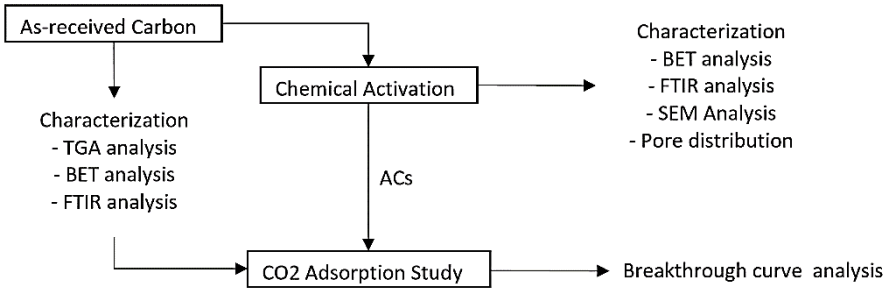

Fig. 1: Overall workflow of the study

$$Fixed\ carbon\ content\ (\%) = 100 - moisture\ content(\%) - volatile\ matter\ (\%) - ash\ content\ (\%) \quad (1)$$

Surface Area and Pore Size Analysis

The specific surface area of ACs was characterized using Brunauer Emmett Teller analyzer (BET) (Micrometritic 3Flex, GA, USA) at 300℃ (degas temperature) for 3 hours. The gas adsorption (N_2) was measured in a vacuum for 3 hours with automated degassed. The heating rate for this analysis is 10℃/min with a sample density of 1.000 g/cm^3. The pore size distribution (PST) of ACs was calculated via density functional theory (DFT) using DFT software from Micrometritic.

Surface Morphology Analysis

The morphology and microstructure of ACs were investigated using Scanning Electron Microscopy (SEM) (Hitachi SU3500, Tokyo, Japan). The image of gold-coated ACs was recorded under a voltage of 10kV and a magnification of 500x.

Functional group analysis

Perkin Elmer Spectrum One FTIR Spectrometer (Thermo Scientific, Ontario, Canada) was used to determine the chemical bonds of the as-received carbon and the produced ACs. The ACs were mixed with KBr powder in a 1:10 ratio and pressed using a force gauge. The spectra were collected at 25℃ with a spectral resolution of 1 cm^{-1} over the spectral range extending from 4000 to 500 cm^{-1}.

CO_2 Adsorption using AC

The adsorption of CO_2 on the produced ACs was conducted through a breakthrough study in a CO_2 adsorption unit shown in Figure 2. 1g of the ACs (700℃, 1:1) was placed in the adsorption unit. Then an inlet gas containing CO_2 and helium (He) flowed into the adsorption unit at of 30℃. The concentrations of CO_2 were measured in both inlet and outlet gas streams every 10 s using a CO_2 gas analyzer. Then the data was plotted to determine the adsorption capacity, represented by breakthrough curves (C_t/C_o vs. t). C_t/C_o is a dimensionless factor, with C_t representing the percent outlet concentration, C_o denoting the percent initial concentration, and t signifying the reaction time (min). The breakthrough curve indicates how well the adsorbent performs in the presence of CO_2. C_t/C_o is a dimensionless factor, with C_t representing the percent outlet concentration, C_o denoting the percent initial concentration, and t signifying the reaction time (min).

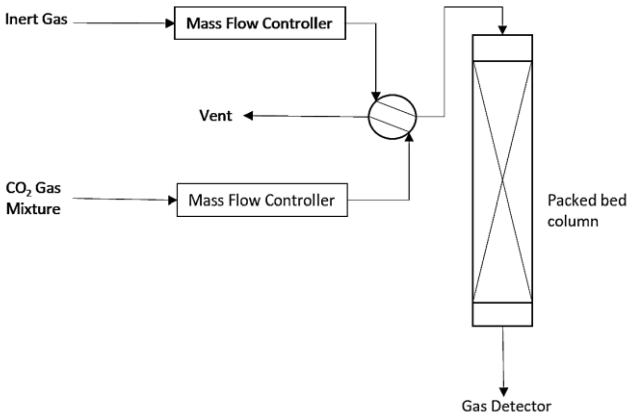

Fig. 2: CO_2 adsorption Unit

RESULTS AND DISCUSSION

Thermal Profile of As-received Carbon

Figure 3 shows the as-received carbon precursor's thermal profile. The analysis was conducted to determine the mass of the carbon as it is heated, cooled, or held at a constant temperature in a defined atmosphere. The mass of the as-received carbon steadily decreased, finally leaving ashes behind. Based on the TGA curve in

Figure 3, pyrolytic thermal degradation of the as-received carbon can be divided into three stages: moisture desorption (below 90°C), main devolatilization, and continuous slight devolatilizationAs-received carbon was estimated to lose approximately 8.6 % of its moisture content (1.633 g). According to Krahnstöver et al. 2016, residual moisture might be one of the possible factors for this phenomenon and can be distinguished from other mass decreases at higher temperatures.

Thermal decomposition of the carbon material occurs through a complex mechanism that is greatly influenced by heat and mass transfer (Momoh et al., 2020). The main devolatilization step released the volatile matter, which ranges from 100°C to 261°C, through the main process at T_p = 206 °C. Based on the result, the mass loss rate was 29.15% or 5.54g. As calculated from the graph, the as-received carbon precursor has 59.68% of the fixed carbon content which signifies the carbonaceous material for the synthesis of ACs.

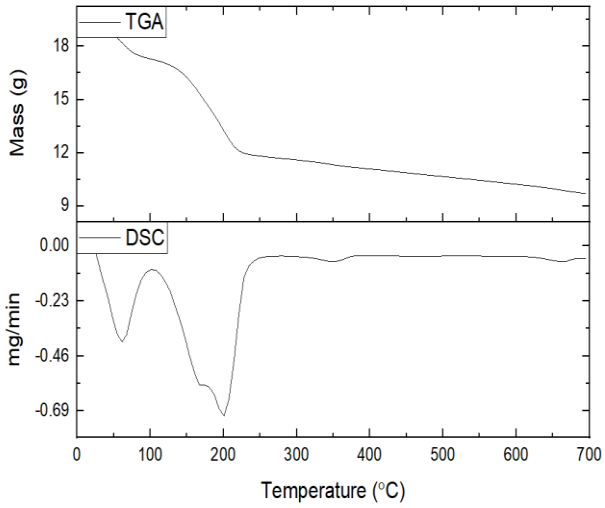

Fig. 3: TGA and DSC curve for as-received carbon

According to Acevedo et al. 2020, the economically profitable raw material might comprise approximately 60% of the carbon content. A high fixed carbon content can produce good ACs (Rodríguezet al., 2010). This is because fixed carbon content provides ACs with a carbon surface that captures the contaminant or adsorbing molecules (Dizbay et al., 2017. Meanwhile, the ash content in the as-received carbon precursor can be revealed by the mass loss at 260 °C to 400 °C, which is about 2.57%. At this rate, the sample mass reaches a nearly constant value corresponding to the sample's ash content. The low ash and high carbon content in carbon waste make it suitable to be used as ACs precursor, as claimed by Prahas et al., 2008.

Surface Area and Pore Size Analysis

Figure 4 illustrates the BET surface area of the ACs treated with different activation temperatures and impregnation ratios. The activation process was conducted at the activation temperatures from 300°C to 700°C, with the carbon to KOH weight ratio varied from 1:1 to 1:5. The obtained result shows that the modified carbon holds a much greater surface area and pore volume compared to the as-received carbon precursor. The as-received carbon persists at 131 m^2/g of surface area with 8.46 $x10^{-2}$ cm^3/g of the total pore volume. The results revealed in Figure 4 indicated that the surface area of ACs can be improved with KOH treatment by varying activation temperature and carbon to KOH ratio. The increase in the activation temperature has resulted in an increment in the surface area of ACs. The interaction of carbon to KOH ratio and temperature indicates that different ratios and temperatures contributed to the different optimum surface areas of ACs.

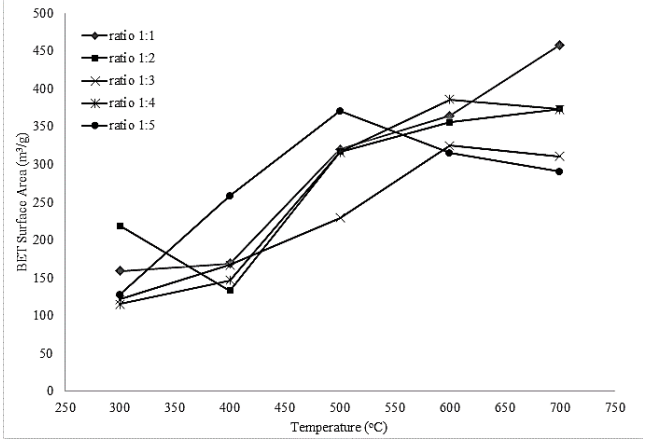

Fig. 4: BET surface area at a different activation temperature

For a low temperature of activation <350°C, a ratio of 1:2 was the optimum condition to reach the high surface area of ACs. While for a moderate temperature of activation 350°C < $T_{activation}$ < 550°C, a ratio of 1:5 gave a higher ACs surface area. On the other hand, for higher activation temperatures (550°C < $T_{activation}$ < 700°C), the ratio of 1:1 was the optimum impregnated condition to give a higher surface area of ACs. From these results, the highest BET surface area of ACs was obtained at the activation temperature of 700°C and impregnated condition of 1:1. At higher temperatures and with the impregnation effect, more pores will be formed within the carbonaceous material, and as a result, a high surface area will be obtained. Pallarés et al., 2018, reported a similar result, who claimed that temperature plays a vital role in the formation of pores on the surface of ACs. Increasing the activation temperature can also encourage the removal of more hydrocarbons and impurities and, thus increase the total pore volume and BET-specific surface area (Huang et al., 2015). The pore size distribution of the developed ACs was calculated from the adsorption–desorption curve using density functional theory (DFT). The relationship between the distribution of the pore volume and pore size is displayed as incremental distributions and accumulation pore volume distribution (Qi et al., 2017). Incremental pore volume for each of the ACs at different carbon-to-KOH ratios and temperature activation is illustrated in Figure 5.

The incremental pore volume with pore size can disclose the pore volume distribution for each pore size. Figure 5 shows that the developed ACs have a uniform pore size distribution, indicating that the adsorbent has a high adsorption capacity due to its high specific surface area and porosity. With an increase in temperature from 300°C to 700°C, each of the employed ratios produced an average pore size of less than 2.327 nm. At 700°C, higher temperatures produce more uniform pores.

The details of the average pore size of the ACs obtained from different activation temperatures are tabulated in Table 1. According to the classification adopted by the International Union of Pure and Applied Chemistry (IUPAC), the adsorbent pores were classified into three groups: micropore (diameter < 2 nm), mesopore (2–50 nm), and macropore (>50 nm) (Saka, 2012). Ilomuanya et al., 2017, also reported that the material with a pore size of less than 2 nm is considered micropore. Thus, these results demonstrate the predominance of micropores and the presence of mesopores.
Nitrogen adsorption is a common technique for analyzing surface area and porous morphologies. The nitrogen adsorption-desorption isotherm for ACs at different temperatures and carbon to KOH ratio 1:1 was illustrated in Figure 6. The analysis data were used to characterize the porosity texture of ACs. Based on the results in Figure 5, the synthesized ACs consist of microporous and mesoporous structures. The results indicate

that ACs treated at 300°C and 700°C have a higher adsorption capacity than another sample at a relative pressure below 0.1, corresponding to micropore filling. The adsorption amount at P/P_o around 0.995 varies from 2.463 mmol/g to 6.397 mmol/g for different samples. The N_2 adsorption-desorption isotherm of each ACs in Figure 4 can be classified as type I isotherms according to the IUPAC adsorption isotherms.

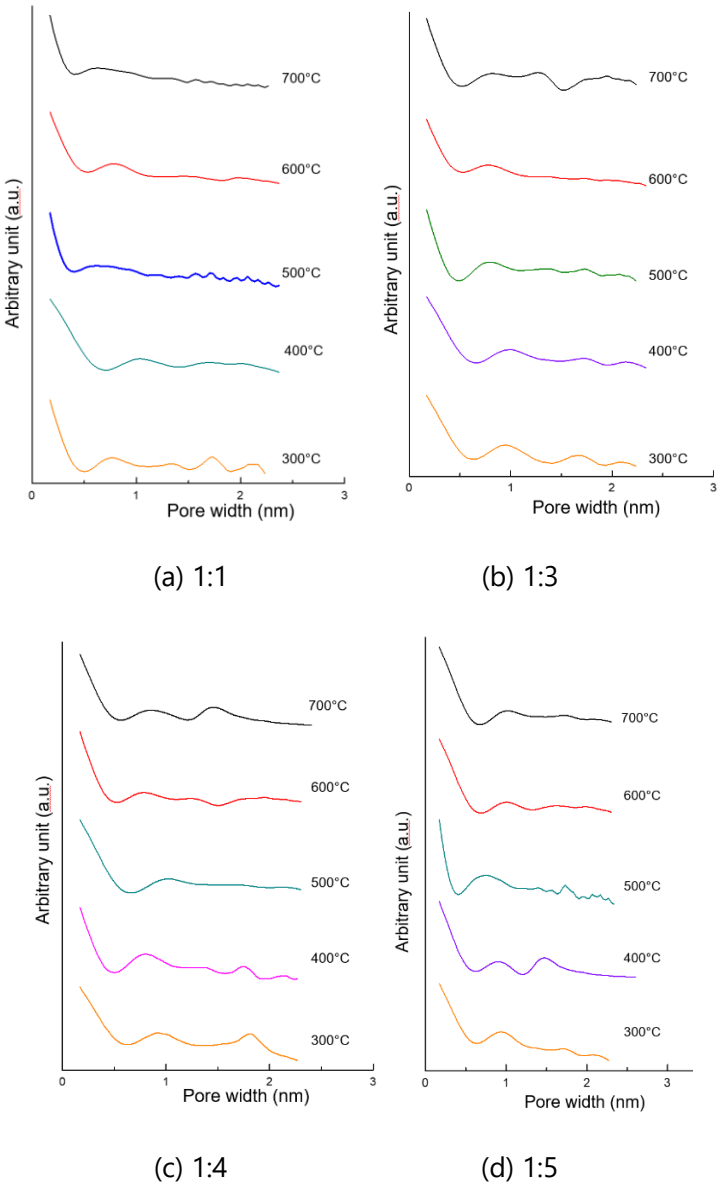

Fig. 5: Pore size distribution (PSD) of ACs calculated from the absorption-desorption curve (DFT) at different ratio carbon/KOH (a) 1:1, (b) 1:3, (c) 1:4, and (d) 1:5.

In the low-pressure region ($P/P_o<0.2$), the adsorption increased due to the micropores filling effect, then a gentle inflection point indicated the formation of a monolayer dispersion. This condition suggests the existence of both mesopores and macropores structures. The hysteresis phenomenon is also observed at low-pressure nitrogen adsorption and usually associated with capillary condensation of adsorption into mesoporous structures (2 – 50nm). The hysteresis loop of the ACs sample in Figure 6 belongs to the type H3 loop, a slit-shaped pore. The unclosed hysteresis loop was observed in each of the ACs samples, even under very low pressure.

Table 1. BET Analysis of as-received carbon precursor and ACs.

Temperature	Impregnation ratio	BET Surface Area (m^2/g)	Micropore, V_{micro} (Å)	Total pore volume (cm^3/g)
As-received carbon	-	131.60	25.71	8.46×10^{-2}
300℃	1:1	158.94	21.23	8.44×10^{-2}
	1:2	218.84	21.69	1.19×10^{-1}
	1:3	121.90	23.01	7.01×10^{-2}
	1:4	115.30	25.75	7.42×10^{-2}
	1:5	127.92	24.64	7.88×10^{-2}
400℃	1:1	168.96	21.78	9.92×10^{-2}
	1:2	133.43	24.93	8.31×10^{-2}
	1:3	166.99	21.90	9.14×10^{-2}
	1:4	146.62	22.50	8.25×10^{-2}
	1:5	258.35	20.34	1.31×10^{-1}
500℃	1:1	319.94	20.15	1.61×10^{-1}
	1:2	316.71	21.07	1.67×10^{-1}
	1:3	229.24	21.48	1.23×10^{-1}
	1:4	316.17	19.51	1.54×10^{-1}
	1:5	370.86	20.37	1.89×10^{-1}
600℃	1:1	364.39	20.43	1.86×10^{-1}
	1:2	355.71	20.12	1.79×10^{-1}
	1:3	324.71	20.99	1.70×10^{-1}
	1:4	385.96	19.95	1.83×10^{-1}
	1:5	315.05	20.39	1.61×10^{-1}
700℃	1:1	458.15	19.29	2.21×10^{-1}
	1:2	373.86	19.92	1.86×10^{-1}
	1:3	310.60	21.03	1.63×10^{-1}
	1:4	372.86	20.34	1.90×10^{-1}
	1:5	290.60	19.67	1.43×10^{-1}

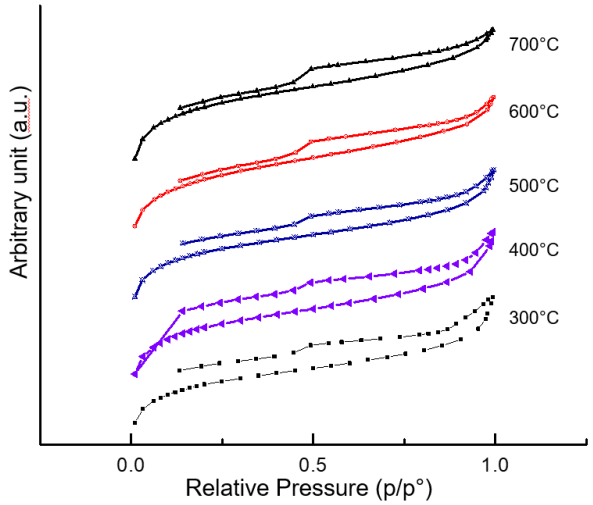

Fig. 6: Nitrogen adsorption-desorption isotherm of ACs at different temperatures.

The reason for this scenario might be because the precursor itself is not a rigid structure and may deform, induced by adsorption or pore-filling (Cai et al., 2014) and the trapped nitrogen cannot be released because of the affinity of nitrogen in the coal caused by the heterogeneous property of the coal surface (Tang et al., 2015). The comprehensive data on the effect of temperature and impregnation ratio on the development of the AC pores are summarized in Table 1.

Surface morphology study

The surface morphology of KOH-impregnated ACs is revealed in the SEM micrographs, as illustrated in Figure 7. The ACs with the highest pore (700°C and carbon to KOH ratio 1:1) were observed and evaluated in the present work. Generally, treated ACs' morphology was improved compared to the as-received carbon. It was observed that the surface of ACs was coarse, implying the existence of mesopores and micropores. The pore structures are developed on the surface of AC with irregular circular structures. According to Zulkurnai et al., 2017, a well-developed pore was required to obtain a large surface area and pore structure, which allowed and facilitated CO_2 adsorption. With the aid of the temperature during activation, the pores formed in the carbon will allow a good distribution of KOH molecules and increase the KOH–carbon reactions. As a result, more pores will be created, enhancing the surface area and pore volume of the ACs (Joshi et al.,2014). Stavropoulos and Zabaniotou et al., 2015 reported that KOH is dehydrated to K_2O, which reacts with CO_2 to give K_2CO_3. The intercalation of metallic potassium appeared to result in the drastic expansion of the carbon material. Thus, the material's large surface area and high pore volume were formed. Additionally, throughout the activation process, the breakdown of material in the precursor owing to heat expansion also causes pore growth. Saka et al., 2012 also stated that the porous structure was generated from the devolatilization process of the organic volatiles, leaving the ruptured surface of ACs with more pores. This finding indicated that chemical activation preferably creates a well-propagated microporous structure inside the raw material particles, allowing the identification of an acceptable adsorption surface.

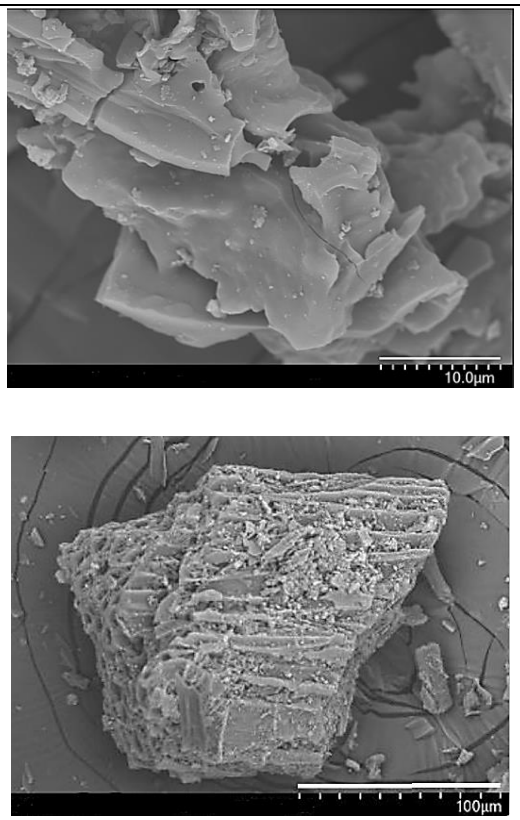

Fig. 7: Surface morphology of (a) as-received carbon (b) activated carbon at 700°C

Functional Group Analysis

The Fourier Transform Infrared (FTIR) spectra for the as-received carbon and ACs at different temperatures and 1:1 ratio of carbon to KOH are illustrated in Figure 8. The results show that the main chemical functional groups that are present in the as-received carbon precursor were C-H stretching and vibration of -OH stretching (3350 - 3200 cm^{-1}), C-O stretching vibration (1577 cm^{-1}), and C-C stretching of the aryl group (1031 cm^{-1}). A similar finding was reported by Melliti et al., 2021. The functional group present in the graph has been shifted from the activation of ACs at different temperatures. However, the characteristic absorption peaks of the ACs almost similar, although the intensity of the absorption peak gradually decreased as the temperature increased. The results indicate that the FTIR spectra of ACs produced at 700°C with a 1:1 impregnation ratio and 2 hours activation time consist of alcohol (O-H stretch bond) at wavenumber 3525 cm^{-1}, aliphatic C-H stretch at 2925 cm^{-1}, and C-H methyl at 1384 cm^{-1}.

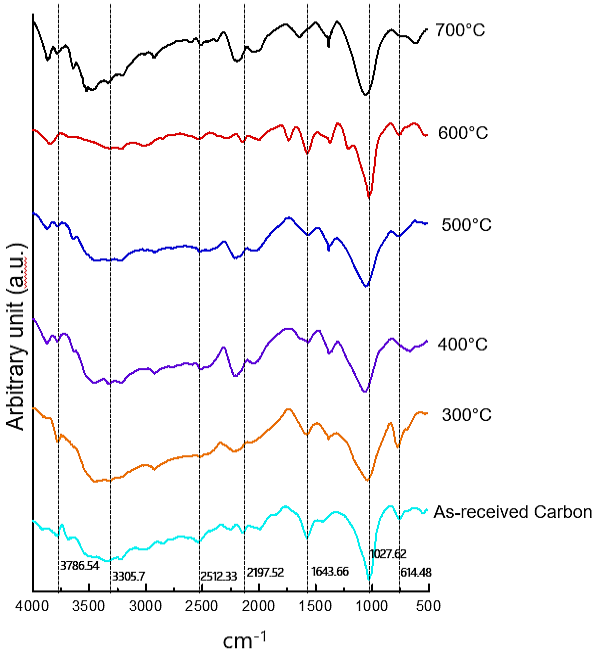

Fig. 8: FTIR spectra of As-received carbon and ACs at different temperature

In addition, the presence of the C=O and C-O stretching between 1640 – 1750 cm^{-1} is attributed to the phenolic ester, carboxylic acid, and conjugated ketonic structures. Meanwhile, the weak band appeared at the peak of 614 cm^{-1} indicating C-H or O-H group. This implied that activation caused some surface changes and removed oxygen-containing functional groups. The obtained spectra are quite similar to those Zulkurnai et al., 2017. According to Pallarés et al., 2018, these properties can greatly affect the adsorption capacity of different pollutants. The result has shown no significant changes in the main functional group of ACs, and is comparable with the as-received carbon.

CO_2 adsorption and Breakthrough curve

A breakthrough curve was plotted for the adsorption of CO_2 using the designed ACs and as-received carbon, as illustrated in Figure 9. This study compared the ACs with the highest surface area (700°C and 1:1) with as-received carbon. In the CO_2 adsorption study, the mixture of gases enters a defined bed of ACs, the CO_2 is absorbed, and the air is passed out of the bed free from the vapor. The process will reach saturation once the vapor is detected in the effluent gas and its concentration is further increased. No further adsorption will occur of this condition, and the composition at the outlet gas is equal to the entry or inlet gas. The result for the ACs at conditions 700°C and 1:1 reveals that the breakthrough curves were skewed in shape, being steeper at the beginning of the curve. Heterogeneity with the bed caused by differences in packing density within the bed, for both macroscale and microscale, is one of the reasons for this skewed shape curve. This is because of the pore size distribution of the carbon particle, from the narrowest of the micropores to the mesoporosity. A higher CO_2 concentration was observed at a low concentration of C_t/C_o in the initial stage process. Moreover, a high mass transfer was noticeable at the inlet, and this might be because the inlet point was the first point of contact between CO_2 gas and the adsorbent in the column. However, as the sorbent got saturated, there was a gradual reduction in mass transfer (García et al., 2011). The steep nature of these curves represents an efficient use of the adsorbent in dynamic processes, in line with a high rate of adsorption (Serna et al., 2010).

In contrast, a flatter concave shape was obtained for as-received carbon, and a longer adsorption time to reach the feed composition was observed. Compared to as-received carbon, which had a breakthrough time of 80 sec, ACs at 700°C likewise had a comparatively quick breakthrough time of 70 sec. The results demonstrated that the chemical activation at 700°C enhanced the surface chemistry of the ACs and increased

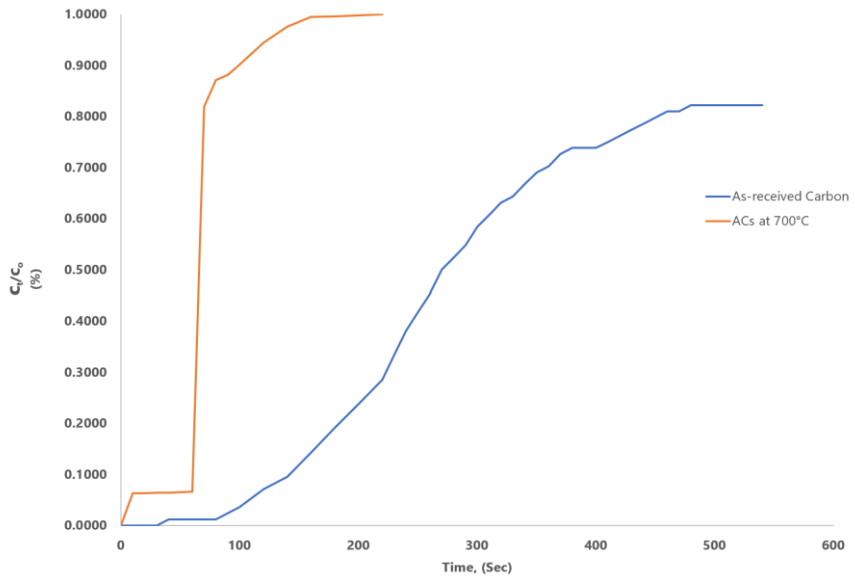

Fig.9: Breakthrough curve

CO_2 molecule binding to the ACs' active sites. This indicates that the treatment has improved the surface chemistry of the ACs and increased the binding of CO_2 molecules to the active sites of the ACs. This observation follows the expected trend as reported by Tan et al. 2008. The adsorption capacity obtained from ACs at 700°C was 0.175 mml/g. From another finding in the AC adsorbent, the highest adsorption capacity obtained was 0.856 mmol/g at 1159 sec (Hazimah et al., 2018), 0.958 mmol/g at 1152 sec (Zulkurnai et al., 2017), and 0.900 mmol/g at 200 minutes (Chowdhury et al., 2013). However, this study's CO_2 adsorption capacity and time could be higher than the current finding. This might be due to the available surface area of the sorbent and the volume of the adsorbent used in the study.

CONCLUSIONS

In this research, as-received carbon from the carbide industry can be utilized as the precursor for ACs synthesis. The characteristic chemical analysis of the as-received carbon indicated that it has approximately 60% fixed carbon content. This study's activation process with KOH produced ACs with a well-developed porosity, consistent with the pore size and surface area of 458.15 m^2/g. The effect of the temperature and impregnation on the ACs formation shows that a higher temperature of 700°C and a ratio at 1:1 gave the highest surface area of ACs. N_2 adsorption-desorption isotherm analysis indicated that the produced ACs consist of micropores, mesopores, and macropores. The coarse surface area with irregular pore structure was formed in the developed ACs, and the oxygen functional groups are more of the chemical group observed in the developed ACs. The adsorption capacity of CO_2 in this study using the developed ACs was found to be 0.175 mmol/g with a breakthrough time of 70 sec. This indicated the binding ability of the CO_2 molecules to the active sites of the ACs. These results suggest that the development of porous structure (microporous or mesoporous fraction) of ACs from as-received carbon from the carbide industry can be used in CO_2 adsorption. However, from a practical point of view, the potential of reusability of the synthesized sorbents and enhancement of porosity should be considered in future studies.

ACKNOWLEDGEMENT

The author is gratefully acknowledged to Universiti Teknologi MARA (UiTM) for financially and technically supporting this research under 600-RMC/GPK 5/3 (180/2020), 600-RMC/GPK 5/3 (149/2020), and 600-IRMI/DANA 5/3/BESTARI (129/2018). The author also would like to thank College of Engineering and School of Chemical Engineering for their continuous support in the research development and internal fund. A high appreciation to the Malaysia Ministry of Higher Education for the continuous support in academic research.

NOMENCLATURE

c_o : The percent initial concentration

c_t : the percent outlet concentration

REFERENCES

Acevedo, S., Giraldo, L., Moreno-Piraján, J. C., 2020. ''Adsorption of CO_2 on activated carbons prepared by chemical

activation with cupric nitrate." *ACS Omega, 5*, 10423–10432.

Cai, Y., Liu, D., Pan, Z., Yao, Y., Li, J., Qiu, Y., 2013. "Pore structure and its impact on CH_4 adsorption capacity and flow capability of bituminous and subbituminous coals from Northeast China." *Fuel, 103*, 258-268.

Chowdhury, Z. Z., Zain, S. M., Rashid, A. K., Rafique, R. F., Khalid, K., 2013. "Breakthrough curve analysis for column dynamics sorption of Mn(II) ions from wastewater by using *Mangostana garcinia* peel-based granular-activated carbon." *Journal of Chemistry, 2013*, 1-8.

Dizbay-Onat, M., Vaidya, U. K., Lungu, C. T., 2017. ''Preparation of industrial sisal fiber waste derived activated carbon by chemical activation and effects of carbonization parameters on surface characteristics.' Industrial Crops and Products, 95, 583–590.

García, S., Gil, M. V., Martín, C. F., Pis, J. J., Rubiera, F., Pevida, C., 2011. "Breakthrough adsorption study of a commercial activated carbon for pre-combustion CO_2 capture," Chemical Engineering Journal, 171, 549–556.

Hazimah, M., Wan Azlina, W. A. K. G., Thomas, C. S. Y., 2018. ''Carbon dioxide adsorption on activated carbon hydrothermally treated and impregnated with metal oxides." Jurnal Kejuruteraan, 30, 31–38.

Huang, P. H., Cheng, H. H., Lin, S. H., 2015. ''Adsorption of carbon dioxide onto activated carbon prepared from coconut shells." Journal of Chemistry, 106590, 1-10.

Hussin, F., Aroua, M. K., Roziki, M. Z. A., Yusoff, R., 2020. ''Carbon dioxide adsorption using biomass-based activated carbon functionalized with deep eutectic solvents.' IOP Conference Series: Materials Science and Engineering, 778, 012169.

Ilomuanya, M., Nashiru, B., Ifudu, N., & Igwilo, C., 2017. ''Effect of pore size and morphology of activated charcoal prepared from midribs of Elaeis guineensis on adsorption of poisons using metronidazole and Escherichia coli O157:H7 as a case study." *Journal of Microscopy and Ultrastructure, 5*, 32-38.

Jatinder, K. R., Manjeet, K., Bharadwaj, A., 2019. ''Synthesis of activated carbon from agricultural waste using a simple method: Characterization, parametric and isotherms study." *Materials Today: Proceedings, 5*, 3334 - 3345.

Joshi, S., Pokharel, B. P., 2014. ''Preparation and characterization of activated carbon from Lapsi (*Choerospondias axillaris*) seed stone by chemical activation with potassium hydroxide." *Journal of the Institute of Engineering, 9*, 79–88.

Khalili, N. R., Campbell, M., Sandi, G., Goals, J., 2000. ''Production of micro- and mesoporous activated carbon from paper mill sludge: I. Effect of zinc chloride activation." *Carbon, 38*,1905 – 1915.

Krahnstöver, T., Plattner, J., Wintgens, T., 2016. ''Quantitative detection of powdered activated carbon in wastewater treatment plant effluent by thermogravimetric analysis (TGA)." *Water Research, 101*, 510–518.

Melliti, A., Srivastava, V., Kheriji, J., Sillanpää, M., Hamrouni, B., 2021. ''Date Palm Fiber as a novel precursor for porous activated carbon: Optimization, characterization and its application as Tylosin antibiotic scavenger from

aqueous solution." *Surfaces and Interfaces, 24,* 101027.

Momoh, E. O., Osofero, A. I., Felipe, A. M., Hamzah, F., 2020. ''Physico-mechanical behaviour of oil palm broom fibres (OPBF) as eco-friendly building material." *Journal of Building Engineering,* 30, 101208.

Nahil, M. A., Williams, P. T., 2012. ''Pore characteristics of activated carbons from the phosphoric acid chemical activation of cotton stalks." B*iomass Bioenergy, 37,*142–149.

Nassima, B., Sandrine, D-O., Lamia, K., Farouk, B., Farida, A-B., Mickaël, G., 2017. ''Single and mixture adsorption of clofibric acid, tetracycline and paracetamol onto activated carbon developed from cotton cloth residue." *Process Safety and Environmental Protection, 111*, 544-559.

Pallarés, J., González-Cencerrado, A., Arauzo, I., 2018. ''Production and characterization of activated carbon from barley straw by physical activation with carbon dioxide and steam." *Biomass and Bioenergy, 115,* 64–73.

Prahas, D., Kartika, Y., Indraswati, N., Ismadji, S., 2008. ''Activated carbon from jackfruit peel waste by H_3PO_4 chemical activation: Pore structure and surface chemistry Characterization." *Chemical Engineering Journal, 140*, 32–42.

Qi, L. L., Tang, X., Wang, Z. F., Peng, X. S., 2017. ''Pore characterization of different types of coal from coal and gas outburst disaster sites using low temperature nitrogen adsorption approach." *International Journal of Mining Science and Technology, 27*, 371-377.

Ramonna, I. K., Athanasios, C. M., George, Z. K., 2019. ''Synthesis of activated carbon from food waste." *Environmental Chemistry Letters, 17*, 429 – 438.

Rodríguez Arana, J. M. R., Mazzoco, R. R., 2010. ''Adsorption studies of methylene blue and phenol onto black stone cherries prepared by chemical activation." *Journal of Hazardous Materials, 180*, 656–661.

Saka, C., 2012. ''BET, TG-DTG, FT-IR, SEM, iodine number analysis and preparation of activated carbon from acorn shell by chemical activation with $ZnCl_2$." *Journal of Analytical and Applied Pyrolysis, 95,* 21–24.

Serna-Guerrero, R., Sayari, A., 2010. '' Modeling adsorption of CO_2 on amine-functionalized mesoporous silica. 2: Kinetics and breakthrough curves." *Chemical Engineering Journal, 161,* 182–190.

Seyyedeh, M. K., Mohsen, S., Mojtaba, J., Tobias, R., Anita, P., Nourollah, M., 2021. ''Pretreatment of lignocellulosic waste as a precursor for synthesis of high porous activated carbon and its application for Pb (II) and Cr (VI) adsorption from aqueous solutions." *International Journal of Biological Macromolecules, 180*, 299-310.

Seyyedeh, M. K., Nourollah, M., Mohammad, M. D., Mohsen, S., 2020. ''A novel post-modification of powdered activated carbon prepared from lignocellulosic waste through thermal tension treatment to enhance the porosity and heavy metals adsorption." *Powder Technology, 366,* 358 – 368.

Stavropoulos, G. G., Zabaniotou, A. A., 2005.

''Production and characterization of activated carbons from olive-seed waste residue." *Microporous and Mesoporous Materials, 82*, 79–85.

Sych, N. V., Trofymenko, S. I., Poddubnaya, O. I., Tsyba, M. M., Sapsay, V. I., Klymchuk, D. O., Puziy, A. M., 2012. ''Porous structure and surface chemistry of phosphoric acid activated carbon from corncob." *Applied Surface Science, 261*,75–82.

Tan, I. A. W., Ahmad, A. L., Hameed, B. H., 2008. Adsorption of basic dye using activated carbon prepared from oil palm shell: batch and fixed bed studies." *Desalination, 225,* 13–28.

Tang, X., Wang, Z., Ripepi, N., Kang, B., Yue, G., 2015. ''Adsorption affinity of different types of coal: mean isosteric heat of adsorption" *Energy Fuels, 29*, 3609-3615.

Wang, K., Li, C., San, H., Do, D. D., 2007. ''The importance of finite adsorption kinetics in the sorption of hydrocarbon gases onto a nutshell-derived activated carbon." *Chem. Eng. Sci., 62,* 6836–6842.

Zulkurnai, N. Z., Mohammad Ali, U. F., Ibrahim, N., Abdul Manan, N. S., 2017. ''Carbon dioxide (CO_2) adsorption by activated carbon functionalized with deep eutectic solvent (DES)." *IOP Conference Series: Materials Science and Engineering, 206*, 012001.